



HAL
open science

Correction to the Taylor hypothesis in swirling flows

J.-F. Pinton, R. Labbé

► **To cite this version:**

J.-F. Pinton, R. Labbé. Correction to the Taylor hypothesis in swirling flows. Journal de Physique II, 1994, 4 (9), pp.1461-1468. 10.1051/jp2:1994211 . jpa-00248055

HAL Id: jpa-00248055

<https://hal.science/jpa-00248055>

Submitted on 4 Feb 2008

HAL is a multi-disciplinary open access archive for the deposit and dissemination of scientific research documents, whether they are published or not. The documents may come from teaching and research institutions in France or abroad, or from public or private research centers.

L'archive ouverte pluridisciplinaire **HAL**, est destinée au dépôt et à la diffusion de documents scientifiques de niveau recherche, publiés ou non, émanant des établissements d'enseignement et de recherche français ou étrangers, des laboratoires publics ou privés.

Classification
Physics Abstracts
47.27 — 47.52 — 47.53

Correction to the Taylor hypothesis in swirling flows

J.-F. Pinton ⁽¹⁾ and R. Labbé ^(1,2)

⁽¹⁾ Ecole Normale Supérieure de Lyon, URA CNRS 1325, 69364 Lyon, France

⁽²⁾ Universidad de Santiago de Chile, Casilla 307, Correo 2, Santiago, Chile

(Received 15 March 1994, received in final form 19 May 1994, accepted 24 May 1994)

Abstract. — We present experimental results on the analysis of turbulent velocity measurements in the flow that develops in the gap between two coaxial counter-rotating disks (von Kármán swirling flow). In the absence of a well-defined mean velocity we introduce the use of a “local Taylor hypothesis” to obtain spatial information from hot-wire measurement at a fixed location. The results are in agreement with conventional open-flow experiments.

1. Introduction.

New interest has emerged for the study of the flow between rotating disks – known as Kármán swirling flows [1-3]. The reason is that when both disks rotate in opposite directions a high Reynolds number flow can be obtained in a compact region of space. This convenient experimental set-up has recently lead to interesting results such as the visualization of vortex filaments [4] and pressure measurements [5]. However, in the analysis of turbulent flows emphasis has traditionally been on velocity measurements with the difficulty that most theoretical (exact or heuristic) predictions are made in the *spatial* domain $v(t \text{ fixed}, x)$ whereas experimental measurements are performed in the *time* domain $v(t, x \text{ fixed})$. For example, Kolmogorov's 1941 similarity theory yields an energy spectrum that, in the inertial range $1/L < k \ll 1/\eta$, scales as $k^{-5/3}$ in the space domain but as ω^{-2} in the time domain – L is the integral length scale and η the dissipation one. Transition between the two domains involves the Taylor hypothesis [6]: if the velocity is sampled at a constant rate Δt at a fixed point of space, the resulting time series $\{v(t_i), t_1 = t_0 + \Delta t, t_2 = t_0 + 2\Delta t, \dots\}$ is converted into a corresponding spatial series: $\{v(x_i) \equiv v(t_i = x_i/U)\}$. This scheme is possible in experiments performed in conditions where the large scale average velocity does not vary appreciably (in grid generated turbulence, for example, the fluctuations are of a few percent) but is open to question in other experimental set-ups such as jets where the fluctuations can be as high as 30 percent or more. It is certainly not applicable in situations where a steady mean flow does not exist at all and this has seriously limited the study of turbulent closed flows in the past.

We note that remarks along similar lines were made long ago, first by Fisher and Davies [7] who have shown experimentally that the convection velocity of inertial range eddies fluctuates as a result of large scale variations of the mean flow, then by several authors – a review may be found in Tennekes and Lumley [8]. However, the purpose of these authors was to *interpret* the time spectra of Eulerian velocity measurement, that is the analysis was made in Fourier space and restricted to flows with some mean velocity. For example Tennekes [9] developed a model in terms of Doppler broadening ($\omega = k\bar{v}$) to explain discrepancies in the position of the viscous dissipative scale as deduced by Lagrangian or Eulerian spectra; this is a phase modulation effect which however small is virtually impossible to deconvolve back to real space. On the contrary, the approach described in this paper is to transform immediately the time series into a spatial series using direct information on large scale velocity variations; the resulting spatial series may then be analyzed conventionally. For this purpose we use a local implementation of the Taylor hypothesis.

2. Experimental set-up.

Air is the working fluid. We use two aluminum horizontal coaxial disks of radius $R = 10$ cm, a variable distance $H = 25$ cm apart – see figure 1. The disks are fitted with a set of 4 vertical blades of height $h_b = 2$ cm and thickness 0.5 cm. Each disk is driven by an independent d.c. motor, whose rotating frequency f is adjustable from 10 to 45 Hz and controlled by a feed-back loop. As observed by previous authors [4, 5, 10] it is thus possible to obtain a turbulent flow with a high Reynolds number. We shall prefer the use of the Reynolds number based on the Taylor scale R_λ since the presence of blades on the disks, not accounted for in the calculation of R_e , plays an important role in the degree of turbulence in the flow. Using 4 blades, we obtained

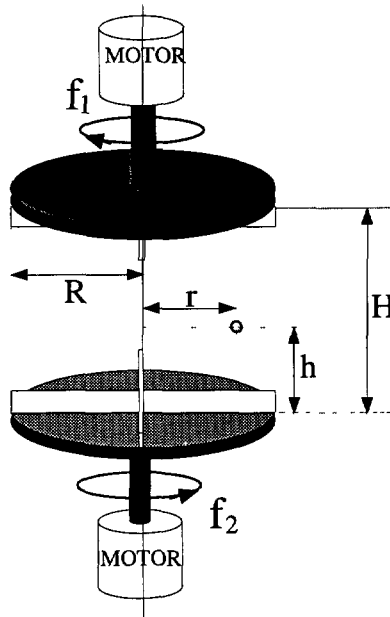


Fig. 1. — Experimental set-up. The working fluid is air. $R = 10$ cm, H is adjustable from 0 to 60 cm (r, h) are the coordinates of the hot-wire probe.

$R_\lambda \sim 450$ with the disks counter-rotating at 2700 rpm (45 Hz). Velocity measurements are performed using a TSI hot-film 10 μm thick and 3 mm long whose position is adjustable. The probe is connected to a TSI 1750 anemometer. In the experiments, the sensing element is parallel to the rotation axis, so that the measured velocity is $v = \sqrt{v_\theta^2 + v_r^2}$. However, we have checked that our results are independent of the orientation of the probe in agreement with the usual isotropy at small scales for high Reynolds numbers. A National Instrument NB-MIO16-XL 16-bit digitizing card is used to record the signal from the probe and to set the rotation frequencies.

3. A local Taylor hypothesis.

Figure 2 shows a recording of the velocity field at a fixed location inside the space between the counter-rotating disks, the probe being located at $r = 5$ cm from the axis and $h = 7.5$ cm from the upper disk. One can see that it is not possible to define from this graph a mean velocity that is steady over a few periods of rotation of the disks, as expected from the geometry of the flow. Accordingly a direct implementation of the Taylor hypothesis ($x = \bar{v}t$) to relate time measurements at a fixed location to the spatial structure of the flow is not applicable (however if the probe is moved close to the blades, there is a steady mean flow and the Taylor hypothesis is applicable as in [10]). Figure 4a shows the spectrum of the raw data, sampled in the time domain (note the absence of frequency peak corresponding to the rotation of the disks since the probe is located inside the core of the flow). A linear region may be detected with an average slope (-1.59) noticeably shallower than the expected (-5/3) value - Kolmogorov's similarity scaling [11]. This is due to the fact that the spectrum cannot be easily related to a spatial spectrum through $\omega = k\bar{v}$, since \bar{v} varies. However we believe that the essence of Taylor's assumption should be maintained, that is: the small scale structures (in the inertial range) are advected by the large eddies at integral scale. We thus implement a "local Taylor hypothesis", i.e. we relate the velocity at time t to that at location x by:

$$v(t) \rightarrow v(x) \quad x = \int_0^t \bar{v}(\tau) d\tau$$

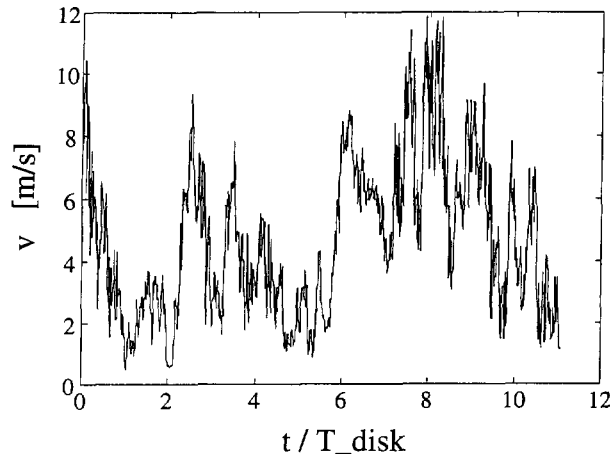


Fig. 2. — Measurement of velocity vs. nondimensional time t/T_{disk} where T_{disk} is the period of rotation of the disks.

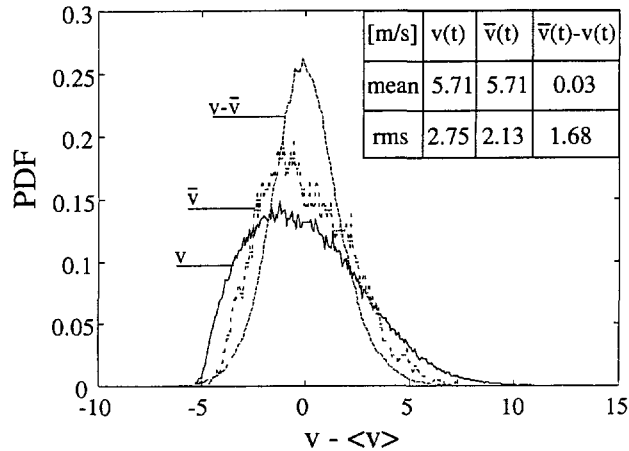


Fig. 3. — Probability density functions of the velocity field $v(t)$, the mean advection velocity $\bar{v}(t)$, and the fluctuations $(v - \bar{v})$.

where \bar{v} is the local average velocity:

$$\bar{v}(\tau) = \frac{1}{T} \int_{\tau-T/2}^{\tau+T/2} v(t) dt$$

where the integral time scale T can be defined quite naturally as the rate at which energy is fed into the flow; in our case, T is the period of rotation of the disks T_{disk} . A local advection velocity defined in this manner has of course the same average value (taken over the entire data record) as the instantaneous velocity; however it is surprising to note that it fluctuates almost as much as the original velocity field – see figure 3, [12]. When the above $v(t) \rightarrow v(x)$ transformation is applied, it produces a series of spatial data, but *unevenly sampled*: when swept by a faster eddy two consecutive time samples correspond to spatial points that are further apart. If care has been taken to oversample the time series, it is possible to resample the spatial series at an even rate, using numerical interpolation. One then obtains a conventional, equally spaced spatial series of the velocity field which may be analyzed as usual. The resulting power spectrum of the energy is shown in figure 4b: one clearly identifies a self-similarity region where $E(k) \propto k^{-1.71}$, a value very close to Kolmogorov's scaling $-5/3$ exponent.

This result is robust with respect to the choice of the integral time T . Indeed when T is varied from $4T_{\text{disk}}$ to $T_{\text{disk}}/4$, the variations of the slope and extension of the scaling region are less than 2.5%. In addition, $T = T_{\text{disk}}$ may be compared to the integral time scale defined from the spectrum of the time series as $1/T_{\text{int}} = [\int f E(f) df] / [\int E(f) df]$. Numerically we obtain $T_{\text{int}} \sim 2T_{\text{disk}}$, that is within the stability range of the algorithm. It also confirms the use of T_{disk} as the characteristic energy injection time. We have also checked that the result is independent of the method used in the numerical resampling scheme if the oversampling factor is sufficient (in our calculation, linear, polynomial and spline interpolations give the same result [13]).

Comparison between figures 4a and 4b shows that one does not only get a better estimate of the slope, the range over which one observes the correct scaling behaviour is larger in the correct space domain and the shape of the cut-off region is changed. Indeed even if observation of figure 4a leads to a scaling exponent of ~ -1.59 , it is possible to find a $-5/3$ scaling region but over a much reduced interval (less than one decade). In contrast figure 4b naturally leads

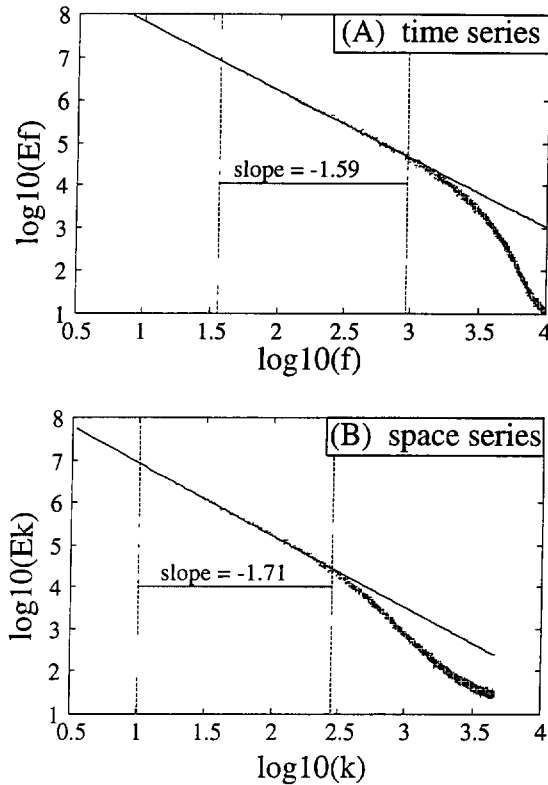


Fig. 4. — a): Power spectrum of time series. b): Power spectrum of resampled spatial series.

to a ~ -1.71 scaling exponent over two decades. We have verified numerically that these effects (shorter scaling range, slightly “humped” cut-off region in the time domain) are due to uneven spatial sampling. Figure 5a (dots) shows a random signal with a $k^{-5/3}$ power spectrum. The solid line corresponds to the same signal but unevenly sampled, that is with Gaussian fluctuations in the sampling interval of amplitude and standard deviation equal to 0.3 (1 is the original sampling frequency). One clearly sees that at small scales the spectrum deviates from the original straight line, starting at a characteristic frequency that decreases with increasing rms value of the fluctuations (note that it explains why the effect has remained unnoticed in experiments with low fluctuations in the mean velocity and wide scaling intervals). Figure 5b is equivalent to the preceding situation but the original spectrum has been terminated with an exponential cut-off (as is believed to be the case in turbulent flows); in the resampling process, the location of the cut-off as well as the sampling interval have been randomized around some average value: one sees that the high frequency end of the spectrum becomes somewhat humped as in experimental observations.

4. Structure functions.

More information about the intermittency characteristics can be gained with the use of the structure functions $SF_p(r) = \langle |v(x+r) - v(r)|^p \rangle$. At a sufficiently high Reynolds number Re , one observes the scaling $SF_p(r) \propto r^{\zeta(p)}$ in the inertial range. The Kolmogorov similarity

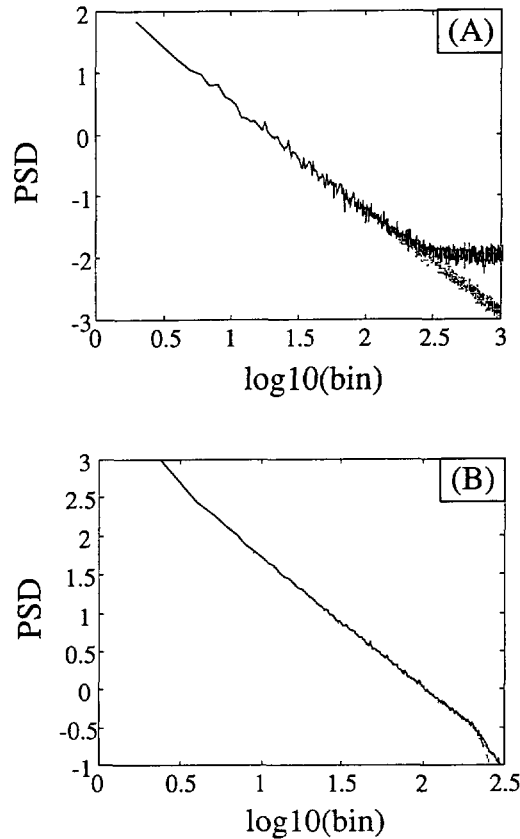


Fig. 5. — Numerical model of the effect of uneven sampling on a signal with a given scaling. a) On the upper graph the spectrum of the original evenly sampled data are represented by a dotted curve, the solid curve is the non uniformly sampled time series. The sampling jitter is Gaussian with amplitude and variance equal to 0.3. b) Same as a) but the original data as an exponential cut-off.

theory implies that in the inertial range $\zeta(p) = p/3$ and deviations from this scaling are usually attributed to intermittency effects. Again it is essential that spatial data be used to relate structure function exponents to usual turbulence analysis. In particular the inertial range is defined correctly only as the region where the Kolmogorov relation $SF_3(r) \propto r$ holds [14, 15]. Figure 6 shows the third order structure functions in each domain. One readily observes a larger linear behaviour in the correct spatial representation, with a slope closer to the expected 1 value. The calculation of the ζ_p exponents should accordingly be done only on data in the spatial domain. We have found $\zeta_2 = 0.72$ and $\zeta_4 = 1.22$ on the resampled spatial series. However for statistical data such as structure functions it is possible to obtain spatial information by directly using the following scheme: first the velocity measurement from the probe is low-pass filtered to get the average velocity \bar{v} over the integral time scale, then the sampling interval of the A/D converter is adjusted to get two successive samples corresponding to a fixed spatial distance Δx : $v_1(t)$ and $v_2(t + \Delta x/\bar{v})$ — the process is now entirely digital and takes 5 ms, i.e. faster than the integral time scale. At this point, the cumulative average of

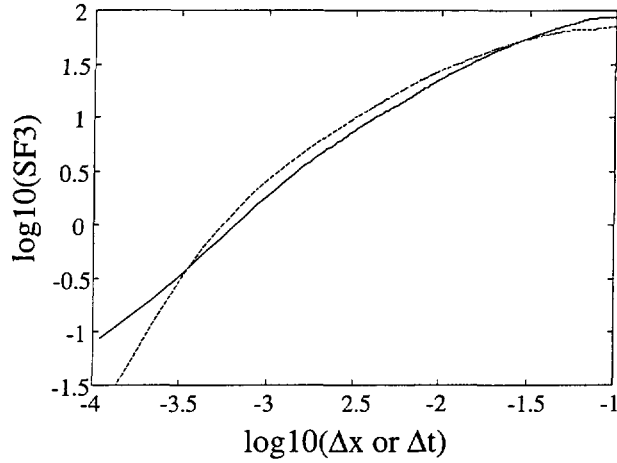


Fig. 6. — Third order structure functions in the space domain (solid line) and in the time domain (dashed line).

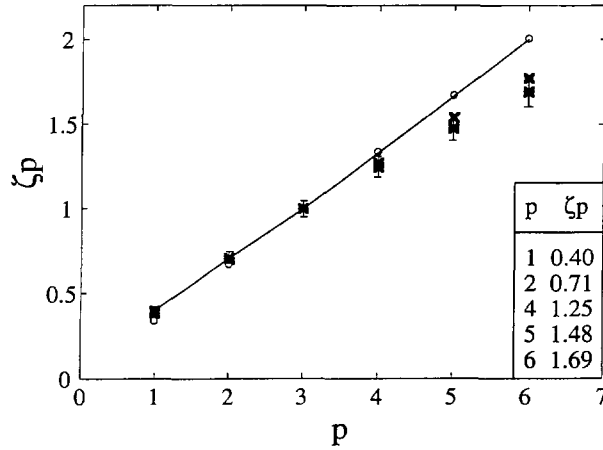


Fig. 7. — Structure function exponents measured directly in the spatial domain using an average velocity controlled sampling interval, compared to standard results: (*) our experiment with counter rotating disks at 35 Hz, (x) wind tunnel measurements of Ciliberto *et al.*, (o) Kolmogorov's $p/3$ dimensional scaling.

$|v_1 - v_2|^p$ can be computed and hence the structure function. Figure 7 shows our results using this method compared to the Kolmogorov prediction and the wind tunnel measurement of Ciliberto *et al.*. We obtain a slightly more intermittent correction but it may not be significant due to the digital nature of the measurement; efforts are currently underway to drive directly (using analog electronic devices) the sampling frequency by the mean velocity.

Finally we have used the ESS technique recently introduced by Benzi and co-workers [16], to plot directly one structure function against another (*the third one, say*). We have found that the scaling exponents take the same values if original time domain data or resampled space domain series are used. We found this result suprising, although a possible explanation might be the following: structure functions are defined in terms of velocity *differences*, so

that neighbouring points in the inertial range (which contribute to the determination of the exponent) are advected at the same large scale velocity and the process is self correcting.

5. Conclusion.

The results presented here on turbulent Kármán swirling flows show how velocity measurements at a fixed location may be analyzed even in the absence of a mean flow. Spatial information is recovered by the use of a local Taylor hypothesis. Our results are coherent with traditional analysis in conventional open-flow geometries. We believe that this method can be extended to the study of other turbulent flows in restricted regions of space [17]. Indeed, such flows can be conveniently used to produce high Reynolds numbers in the laboratory.

Acknowledgments.

The authors thank S. Fauve, S. Ciliberto, C. Baudet and P. Goncalves for many interesting discussions. This work was partly supported by CEE contract CI1*-C91-0947.

References

- [1] von Kármán T., *Zeits. f. angew. Math. u. Mech.* **1** (1991) 244. or *NACA Rep. 1092* (1946).
- [2] Picha K. G., Eckert E. R. G., *Proc. 3rd US Natl. Cong. Appl. Mech.* (1958) pp. 791-798.
- [3] Zandebergen P.J., Dijkstra D., *Ann. Rev. Fluid. Mech.* **19** (1987) 465-491.
- [4] Douady S., Couder Y., Brachet M.-E., *Phys. Rev. Lett.* **67** (1991) 983-986.
- [5] Fauve S., Laroche C., Castaing B., *J. Phys. II France* **3** (1993) 271-278.
- [6] Taylor G.I., *Proc. R. Soc. A.* **164** (1928) 476.
- [7] Fisher M.J., Davies P.O.A.L., *J. Fluid Mech.* **18** (1964) 97-116.
- [8] Tennekes H., Lumley J.L., *A first course in Turbulence* (MIT Press, 1972).
- [9] Tennekes H., *J. Fluid Mech.* **3** (1975) 561-567.
- [10] Maurer J., Tabeling P., Zocchi G., *Europhys. Lett.* **26** (1993) 31-36.
- [11] Kolmogorov A.N., *Dokl. Akad. Nauk. S.S.S.R.* **30** (1941) 301-305.
- [12] Extensive studies are underway regarding the statistical properties of \bar{v} , and related physical quantities. The results will be published in a forthcoming paper.
- [13] It is not strictly necessary to resample the data series to obtain its Fourier spectrum, it can be calculated as the scalar product $f(k) = \langle f(x) | e^{ikx} \rangle$. However it is essential for the calculation of other statistical data, such as moments and structure functions.
- [14] Monin A.S., Yaglom A.M., (MIT Press, 1971).
- [15] Baudet C., Ciliberto S., Phan Nhan Tien, *J. Phys. II France* **3** (1993) 293-299.
- [16] Benzi R., Ciliberto S., Baudet C., Ruiz-Chavarriaz G., *Europhys. Lett.* (1993) in press.
- [17] Turbulent convective flow for example, R. Benzi private communication.